Superheating and Supercooling of Vortex Matter in a Nb Single Crystal: Direct Evidence for a Phase Transition at the Peak Effect from Neutron Diffraction

X. S. Ling,[1] S. R. Park,[1] B. A. McClain,[1] S. M. Choi,[2,3] D. C. Dender,[2,3] and J. W. Lynn[2]

[1]*Department of Physics, Brown University, Providence, Rhode Island 02912*

[2]*NIST Center for Neutron Research, Gaithersburg, Maryland 20899*

[3]*University of Maryland, College Park, Maryland 20742*

(Received 11 August 2000)

We report the first observation of a striking history dependence of the structure function of vortex matter in the peak effect regime in a Nb single crystal by using small angle neutron scattering combined with *in situ* magnetic susceptibility measurements. Metastable phases of vortex matter, supercooled vortex liquid and superheated vortex solid, have been identified. We interpret our results as direct structural evidence for a first-order vortex solid-liquid transition at the peak effect.

DOI: 10.1103/PhysRevLett.86.712 PACS numbers: 74.60.Ge, 61.12.Ex

It was found recently [1] that the equilibrium magnetization jump in high-T_c superconductor $YBa_2Cu_3O_{7-\delta}$ (YBCO), a widely accepted thermodynamic signature of a vortex solid-liquid transition [2], coincides with the peak effect, a well-known anomaly due to vortex-lattice softening and random pinning in many low-T_c [3,4] and high-T_c [1,5,6] superconductors in which the critical current exhibits a peak rather than decreasing monotonically with increasing temperature. However, there is no direct structural evidence indicating whether the underlying phase transition is solid-to-solid, solid-to-liquid, or even liquid-to-liquid in origin. Since quenched disorder is known to have important consequences for phase transitions [7,8], whether a solid-liquid transition can occur in vortex matter has broad implications.

Small angle neutron scattering (SANS) [9–13] is presently the most powerful technique for probing the vortex structure in bulk superconductors. For high-T_c superconductors, however, the vortex SANS signals are too weak (due to the large magnetic penetration depth) for a direct structure study of the peak effect. Recent effort has thus focused on low-T_c systems [12,13]. However, it has been controversial as to whether there is a vortex solid-liquid transition in Nb [12,13]. In an early SANS study [12], the azimuthal width of the Bragg peaks starts to increase with temperature was interpreted as the vortex-lattice melting transition. In another study [13], a nearly isotropic ring of scattering was observed in the peak-effect regime, but was interpreted as a disordered solid rather than a liquid. In both studies, only field-cooled vortex states were measured.

We report here striking hysteresis in neutron diffraction patterns of the vortex state in the peak-effect regime of Nb. The metastability of supercooled and superheated vortex states is directly demonstrated by applying a weak perturbation and observing the evolution of the SANS patterns. These results establish a first-order vortex solid-liquid transition in Nb at the peak effect.

Our experiments were performed using the 30-m SANS instrument NG-7 at the NIST Center for Neutron Research. The increased neutron flux due to a new liquid-hydrogen cold source is important, but the key improvement in the present experiment is that the SANS and the ac magnetic response of the vortex array are measured simultaneously *in situ*. Thus one can correlate the ordering in the vortex state directly with the macroscopic vortex dynamics. The coil for the ac susceptibility measurements is also used to apply an ac field to dynamically perturb the vortex system, allowing an *in situ* determination of the metastability of the vortex states.

The sample is a Nb single crystal of 99.998% purity, a cylinder with a slightly uneven diameter from 1.316 cm at one end to 1.169 cm at the other, and 2.48 cm in length. The incident neutron beam has a mean wavelength $\lambda = 6.0$ Å and a bandwidth $\Delta\lambda/\lambda = 0.11$. The neutron beam traverses through the central region of the sample, defined by a cadmium mask (0.7 cm in diameter), along the cylindrical axis which coincides with the threefold symmetric $\langle 111 \rangle$ crystallographic direction. The dc magnetic field is applied by a horizontal superconducting magnet along the same direction. The absolute accuracy of the measured sample temperature is ± 0.20 K with a temperature stability better than ± 0.025 K.

The peak-effect regime of the Nb sample is determined *in situ* by measuring the characteristic dip in the temperature dependence of the real part of the ac magnetic susceptibility $\chi'(T)$, as shown in Fig. 1(a) for $H = 3.75$ kOe. The pronounced diamagnetic dip in $\chi'(T)$ of the ac susceptibility corresponds to a strong peak effect in the critical current (or nonlinear conductance) in the sample [1,5]. The onset, the peak, and the end of the peak effect are denoted by $T_o(H)$, $T_p(H)$, and $T_{c2}(H)$, respectively. Figure 1(b) shows the window of our experiment.

For each (T, H), we measure the vortex SANS patterns for different thermal paths. For low temperatures the vortex SANS images show sharp Bragg peaks with sixfold symmetry in agreement with previous studies [9,12,13], independent of the thermal history. An example is shown in the inset of Fig. 1(b) for $H = 3.75$ kOe and $T = 3.50$ K. However, the vortex SANS pattern starts to show striking

 0031-9007/01/86(4)/712(4)$15.00

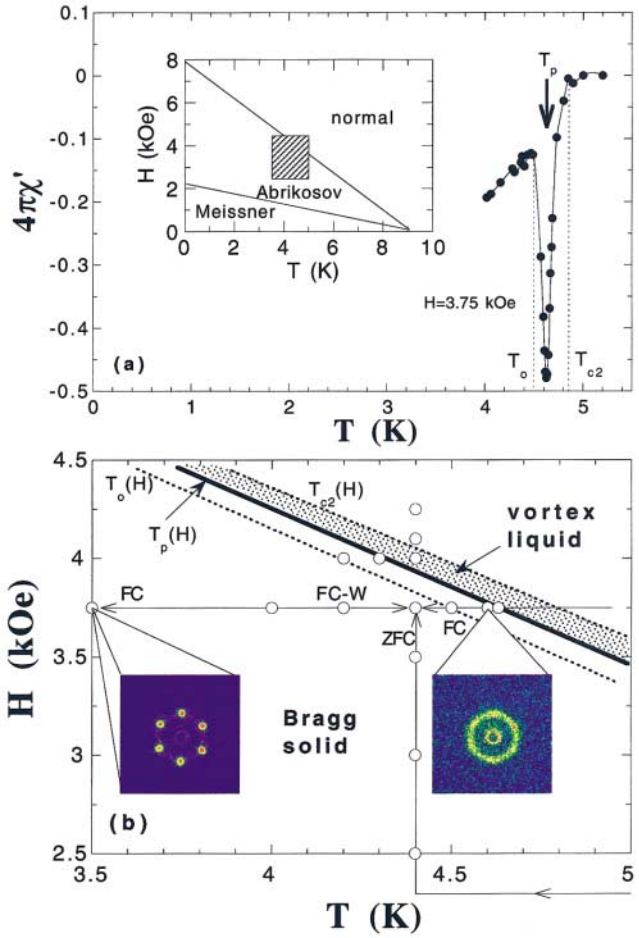

FIG. 1 (color). (a) Magnetic ac susceptibility $\chi'(T)$ vs T for $H_{\rm dc} = 3.75$ kOe. $H_{\rm ac} = 3.3$ Oe and $f = 1.0$ kHz. $H_{\rm dc} \parallel H_{\rm ac}$. (For details on ac magnetic measurements, see [1,5].) Inset: The schematic H-T phase diagram for the Nb crystal used in this study. (b) Expanded view of the H-T phase diagram for Nb [the shaded box in (a)]. The open circles indicate the H-T parameters of this experiment. The SANS images are for field-cooled vortex states (no background subtraction).

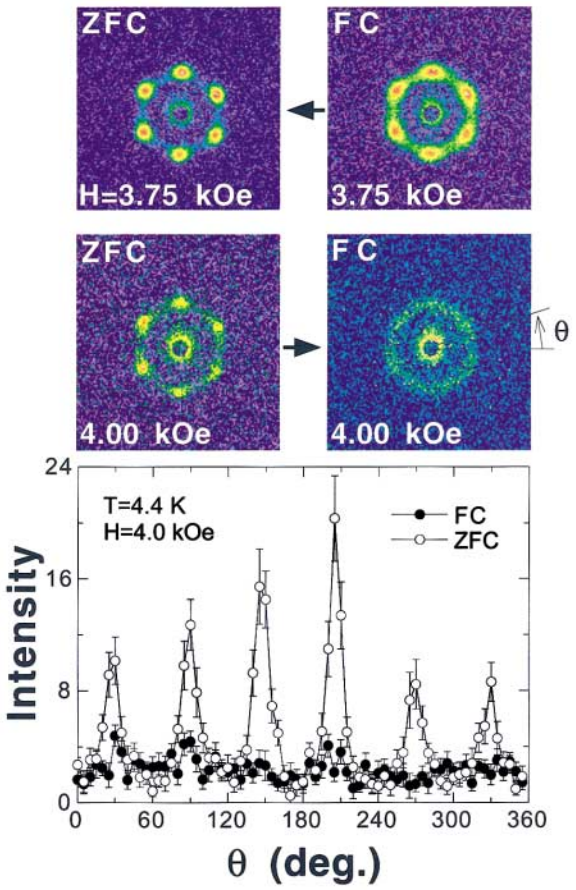

FIG. 2 (color). History-dependent neutron diffraction patterns. $T = 4.40$ K for all images. The SANS images of the ZFC and FC vortex states for $H = 3.75$ kOe (top panel: $T < T_p$) and $H = 4.00$ kOe (middle panel: $T > T_p$). The thick arrows indicate how the SANS images evolve after applying a small ac field (see text). The lower panel shows the intensity data at the radial maximum as a function of the azimuthal angle θ for the ZFC and FC SANS data (background subtracted) at $H = 4.00$ kOe and $T = 4.40$ K.

history dependence as the peak-effect regime is approached. For clarity, we define the field-cooled (FC) state as when the sample is cooled to the target temperature in a magnetic field, while the zero-field-cooled (ZFC) state is reached by cooling the sample in zero field to the target temperature and then increasing the magnetic field to the desired value. A field-cooled-warming (FC-W) state is when the system is cooled in field to a much lower temperature ($\sim$2 K) then warmed back to the final temperature.

For the FC path, the vortex SANS patterns show nearly isotropic rings for $T_p < T < T_{c2}$ and broad Bragg spots for $T < T_p$. There is no clear sharpening in the Bragg peaks when T_o is crossed. Only at a lower T do the Bragg peaks become sharp. In contrast, for the ZFC and the FC-W paths, the sharp Bragg spots are observed for all temperatures up to T_{c2}. Shown in the top panel of Fig. 2 are the ZFC and FC images at $H = 3.75$ kOe and $T = 4.40$ K, which is just below $T_o(3.75\ \text{kOe}) = 4.50$ K. The images in the middle panel are for $H = 4.00$ kOe and $T = 4.40$ K, which is 0.10 K above $T_p(4.0\ \text{kOe}) = 4.30$ K. The intensities at the radial maximum for the middle panel SANS data are plotted in the lower panel. The sharp Bragg spots for the ZFC states indicate long-range order (LRO) [14], while the broad spots for the FC states suggest a disordered phase with short-range order.

The orientational order of the vortex assembly can be quantified by the azimuthal widths of the Bragg peaks at the radial position of the intensity maximum. The azimuthal widths $\Delta\theta$ of the Bragg peaks can be obtained by fitting six Gaussian peaks to the data, for each (T, H) and path. Likewise, the translational order of the vortex assembly can be quantified by the radial widths ΔQ of the Bragg peaks. The Gaussian widths are plotted in Fig. 3. To determine the positional correlation of the vortex lines along the field direction, rocking curves (Bragg peak intensity vs the relative angle between the neutron beam and the magnetic field) of the ZFC and FC states at $H = 3.75$ kOe and $T = 4.40$ K are also measured. The rocking-curve width

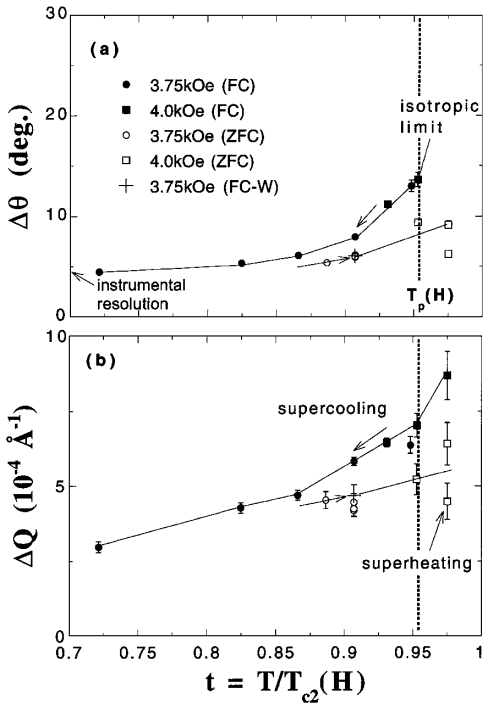

FIG. 3. (a) The azimuthal widths of the Bragg peaks at Q_o and (b) the radial widths vs reduced temperature for ZFC, FC, and FC-W vortex states. The FC-W data points at 3.75 kOe and 4.40 K are indicated by the crosses (and marked by arrows). The lines are guides for the eye. The dashed lines indicate $T_p(H)$.

for the FC state is 30% larger than that of the ZFC state, suggesting that the vortex lines are entangled [15] in the FC states, but nearly straight in the ZFC (and FC-W) states.

Since a simultaneous broadening in radial and azimuthal widths is characteristic of a liquid (or glass) [16], the hysteresis in both $\Delta\theta$ and ΔQ in Fig. 3 suggests a first-order vortex solid-liquid transition. An open issue is the location of the vortex phase transition in the peak effect. One view [4,17,18] places the conjectured vortex solid-liquid transition T_m at T_p, while the other [6,13] places T_m at $T_{c2}(H)$ for Nb. In the latter scenario, the FC disordered phase observed here (as well as in [12,13]) is a supercooled liquid and the thermodynamic ground state is an ordered solid across the entire peak-effect regime, as one might expect from the Lindemann criterion estimate [19], provided the vortex-lattice elasticity is well behaved up to $T_{c2}(H)$.

We find that one can experimentally determine the ground state, and T_m, of the vortex system. For this purpose, we use the ac susceptibility coil to apply a small ac magnetic field to shake the vortex assembly and use the SANS to observe how the structure of the system evolves. Even though the true ground state of the vortex system may not have been reached in the time scale of the experiment, the evolution of the diffraction patterns leaves little doubt regarding the nature of the ground state.

For $T > T_p$, after applying an ac field (3.3 Oe at 100 Hz) for 10^3 sec, the ordered ZFC states become disordered (Fig. 4). Preliminary time-dependent data show that the Bragg peaks start to disappear within the first 10^2 sec of the experiment. In contrast, no measurable difference can be found for the disordered FC states before and after the ac field is applied (for up to 10^4 sec). By using the same approach, we find that the disordered FC states for $T < T_p$ are metastable and the ground state is an ordered lattice, opposite to that for $T > T_p$. In the $T < T_p$ regime, the metastability is obviously stronger since a much larger ac field is needed to change the metastable states. We find that an ac field of 50 Oe (at ≈0.1 Hz, using the superconducting magnet at nonpersistent mode) can crystallize the disordered FC states at $T < T_p$. The shaking effects of an ac magnetic field were observed in transport [20] and ac magnetization [21] in the peak-effect region in 2H-NbSe2, and were interpreted as vortex reordering, consistent with our direct observations here.

The metastable nature of the ordered ZFC states for $T > T_p$ can also be observed in a field ramping experiment. For example, at a field ramp (increase) rate of less than 5 Oe/sec, the final vortex state (at $T > T_p$) is always ordered. In contrast, a ramp rate larger than 40 Oe/sec always results in a disordered state. However, the field ramping experiment alone cannot rule out a trivial possibility that the sample was heated to above $T_{c2}(H)$ during the field ramping by the induced screening current. In this case, once ramping stops, the sample cools back to the

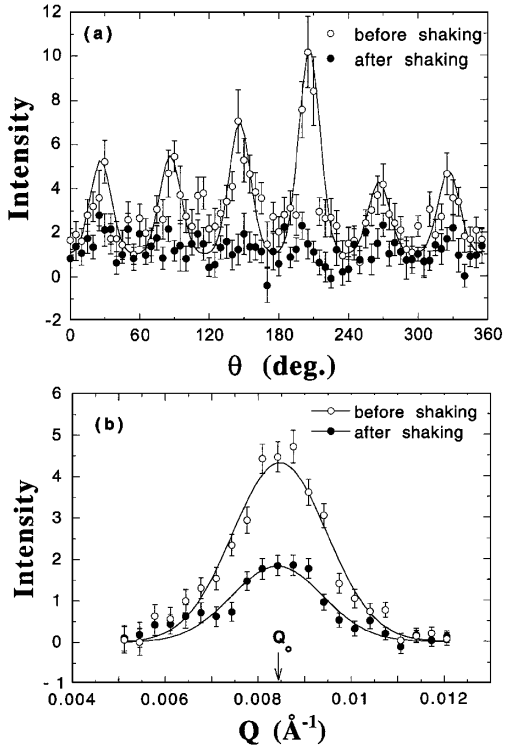

FIG. 4. The effect of an ac field, $H_{ac} = 3.3$ Oe and $f = 100.0$ Hz, on the ordered ZFC state for $H = 4.00$ kOe and $T = 4.40$ K [above $T_p(H)$]. (a) $I(Q_o)$ vs azimuthal angle; (b) the intensity $I(Q)$ (averaged over the azimuthal angle) as a function of the momentum transfer Q. The location of the radial maximum Q_o is found by fitting $I(Q)$ to a Gaussian. The lines are Gaussian fittings.

set temperature *in* field and the final state is actually a FC state. In the shaking experiment, the ac susceptibility of the sample is monitored and serves as an *in situ* thermometer to ensure that the sample temperature never fluctuates to above $T_{c2}(H)$ during the entire SANS run (1 h).

Thus we conclude that, for $T > T_p$, the ordered ZFC vortex lattice is a superheated state and the ground state of the vortex system is a disordered vortex liquid, while for $T < T_p$, the ground state is a vortex Bragg solid [14], and the disordered FC state is a supercooled vortex liquid. A thermodynamic phase transition must have taken place in the region of the peak effect, $T_m \approx T_p$. This is consistent with the observations in YBCO where the magnetization jump was found to coincide with the peak effect [1]. In principle, one should also observe a discontinuous change of Q_o when the vortex solid melts. Unfortunately, the expected shift in Q_o due to the density change at the vortex solid-liquid transition is below our resolution limit, as we estimate here. From thermodynamic considerations [2], using the Clausius-Clapeyron relations, the vortex density change at T_m is of the order $\Delta B = -4\pi c_L{}^2 C_{66}/(T_m dH_m/dT)$ where c_L is the Lindemann number and $C_{66} \approx (B_{c2}^2/4\pi)[b(1-b)^2/8\kappa^2]$ is the vortex-lattice shear modulus, $b = B/B_{c2}$. For Nb at $H = 4.00$ kOe, $T_m \approx T_p = 4.30$ K $(T_{c2} = 4.50$ K), $dH_m/dT = -0.846$ kOe/K, and $C_{66} \approx 0.6 \times 10^4$ erg/cm^3 assuming a reasonable $\kappa \approx 1$ and Lindemann number $c_L = 0.1$, the upper bound for the jump ΔB at melting is about 0.2 G. For a triangular lattice before melting $Q_o(B = H) = 2\pi\sqrt{2/\sqrt{3}}\sqrt{H/\phi_o}$, the expected $\Delta Q_o \approx 3 \times 10^{-5} Q_o$ which is far too small to be resolved by the present SANS instruments. In Fig. 4(b), the radial peak position Q_o remains unchanged after shaking-induced melting, consistent with the above estimate.

Another interesting feature in Fig. 3 is that there appears to be a characteristic temperature below which the vortex state is insensitive to its thermal history. The crossover temperature, $t \approx 0.85$ in Fig. 3, is, in fact, very close to the melting line identified previously [12]. We interpret this temperature as the lower limit for supercooling. A closer examination of the diffuse scattering rings in Figs. 1 and 2 suggests that they are not completely isotropic, indicating some short-range correlations. We attribute this short-range order to the coupling of the vortex liquid to the atomic crystal lattice, since experimentally one finds that in the Bragg solid phase, the specific orientation of the vortex lattice is always fixed to a certain crystallographic orientation of the sample [11]. In the supercooled state (top right in Fig. 2), the highly correlated vortex liquid [12], reminiscent of the hexatic liquid phase in 2D melting [22], may also be related to this coupling.

In conclusion, we have observed the first structural evidence of a first-order vortex solid-liquid transition at the peak effect in a Nb single crystal using a simultaneous SANS and ac magnetization technique. Our observation of shaking induced melting (disordering) resolves a well-known puzzle [23,24] in which the resistance hysteresis always vanishes at $T_p(H)$. Only with extremely low drive currents may one observe the subtle effects of superheating in transport [25]. The superheating of a vortex solid contrasts sharply with that in regular bulk solids where surface melting prevents superheating [26]. Surface melting of a vortex solid is likely suppressed by the surface barrier [25] in type-II superconductors.

We thank C. J. Glinka for assistance and J. J. Rush for providing the Nb crystal, as well as C. Elbaum, A. Houghton, J. M. Kosterlitz, H. J. Maris, and S. C. Ying for discussions. This work was supported by NSF Grant No. DMR-0075838 and the A. P. Sloan Foundation.

[1] J. Shi *et al.,* Phys. Rev. B **60**, R12 593(1999); T. Ishida, K. Okuda, and H. Asaoka, Phys. Rev. B **56**, 5128 (1997).
[2] E. Zeldov *et al.,* Nature (London) **375**, 373 (1995); R. Liang, D. A. Bonn, and W. N. Hardy, Phys. Rev. Lett. **76**, 835 (1996); U. Welp *et al., ibid.* **76**, 4809 (1996).
[3] A. I. Larkin and Yu. N. Ovchinnikov, J. Low Temp. Phys. **34**, 409 (1979); R. Wördenweber, P. H. Kes, and C. C. Tsuei, Phys. Rev. B **33**, 3172 (1986).
[4] S. Bhattacharya and M. J. Higgins, Phys. Rev. Lett. **70**, 2617 (1993).
[5] X. S. Ling and J. I. Budnick, in *Magnetic Susceptibility of Superconductors and Other Spin Systems,* edited by R. A. Hein *et al.* (Plenum Press, New York, 1991), p. 377.
[6] W. K. Kwok *et al.,* Phys. Rev. Lett. **73**, 2614 (1994).
[7] Y. Imry and S.-k. Ma, Phys. Rev. Lett. **35**, 1399 (1975).
[8] D. S. Fisher, M. P. A. Fisher, and D. A. Huse, Phys. Rev. B **43**, 130 (1991).
[9] D. K. Christen *et al.,* Phys. Rev. B **15**, 4506 (1977).
[10] R. Cubitt *et al.,* Nature (London) **365**, 407 (1993).
[11] B. Keimer *et al.,* Phys. Rev. Lett. **73**, 3459 (1994).
[12] J. W. Lynn *et al.,* Phys. Rev. Lett. **72**, 3413 (1994).
[13] P. L. Gammel *et al.,* Phys. Rev. Lett. **80**, 833 (1998).
[14] T. Giamarchi and P. Le Doussal, Phys. Rev. B **52**, 1242 (1995).
[15] D. R. Nelson, Phys. Rev. Lett. **60**, 1973 (1988); M. C. Marchetti and D. R. Nelson, Phys. Rev. B **41**, 1910 (1990).
[16] P. M. Chaikin and T. C. Lubensky, *Principles of Condensed Matter Physics* (Cambridge University Press, Cambridge, 1995).
[17] E. Granato, T. Ala-Nissila, and S. C. Ying, Phys. Rev. B **62**, 11 834 (2000); J. Phys. Condens. Matter **2**, 8537 (1990).
[18] A. I. Larkin, M. C. Marchetti, and V. M. Vinokur, Phys. Rev. Lett. **75**, 2992 (1995).
[19] A. Houghton, R. A. Pelcovits, and A. Sudbø, Phys. Rev. B **40**, 6763 (1989).
[20] M. W. Rabin *et al.,* Phys. Rev. B **57**, R720 (1998).
[21] S. S. Banerjee *et al.,* Appl. Phys. Lett. **74**, 126 (1999).
[22] B. I. Halperin and D. R. Nelson, Phys. Rev. Lett. **41**, 121 (1978).
[23] W. Henderson *et al.,* Phys. Rev. Lett. **77**, 2077 (1996).
[24] X. S. Ling, J. E. Berger, and D. E. Prober, Phys. Rev. B **57**, R3249 (1998).
[25] M. Charalambous *et al.,* Phys. Rev. Lett. **71**, 436 (1993).
[26] F. Lund, Phys. Rev. Lett. **69**, 3084 (1992).